Chapter 4

Molecular Characterization and Wnt Requirements in Polyps Initiated by BMP Dysregulation

4.1 Introduction

The regulation of homeostatic signaling gradients relies on inter-compartmental interactions. Disruption of these intercellular dynamics is enough to alter intestinal function and drive colorectal transformation.

In Hereditary Mixed Polyposis Syndrome (HMPS), a 40kb duplication upstream of GREM1 causes a pathological change in the localization of this transcript: from a restricted mesenchymal gradient to ectopic epithelial gene expression. This alters the polarized gradients of morphogens that maintain intestinal homeostasis and causes a characteristic crypt budding phenotype with the development of Ectopic Crypts (ECF). In 2015, Davis et al recreated this phenotype by expressing the gene *GREM1* under the epithelial promoter Villin to generate the *Vil1-Grem1* (VG) mouse. As described by Davis et al[132], these animals developed ECF within 3 months and presented with a mixed pan-intestinal polyposis by month 7. Importantly, VG lesions showed characteristics of the three morphologies observed in HMPS patients: serrated, adenomatous and cystic. However, the molecular sequence of events through which Gremlin-1 expression drives this phenotype is yet to be established, and some important questions await to be answered. Is disruption of the Bmp gradient enough to compromise the mechanisms that confer Stem Cell (SC) identity? Does disruption of Wnt occur somewhere along the way? Which populations of SC populate the ECF in VG animals? Here, we use a combination of molecular and histological techniques to address these issues and bring a better understanding of BMP-initiated colorectal

tumorigenesis.

4.2 Objectives

- To unveil the molecular sequence of events behind Gremlin-1-driven tumorigenesis.
- To assess the SC composition of Gremlin-1 initiated polyps using the levels of expression of *Lgr5* and *Anxa1* as a surrogates of SC identity.
- To investigate the WNT requirements of BMP-initiated polyposis.
- To compare early and late stages of Gremlin-1 initiated pathogenesis in terms of SC composition and Wnt disruption.

4.3 Histopathological Progression of the Vil1-*Grem1* Pathogenesis

The phenotype of VG animals advances progressively during the first year of life, with signs of pathology being detected already after 3 months [132]. This process begins with the transformation of the villi, which become larger and thicker, with a more abundant stromal compartment than that found in WT animals (Fig. 13B). From the sides of these villi, small proliferative pockets start to form, which are the origin of ECF. By month 3, one can start to observe early polyps forming in the small intestine of VG animals, which are populated by ECF (Fig.13C). By month 6, intermediate polyps (over 2mm) populate the intestines of VG animals, the majority of which show no signs of dysplasia (Fig.13D). However, high grade dysplasia could be observed at edges of a minority (less than 1 percent) of advanced polyps (Fig.13E). Intermediate and advance polyps co-exist in the same samples, and the molecular differences between these two types of lesions remains to be investigated (Fig.1).

4.4 Ectopic Crypts are negative for CBC and RSC markers

As described in the previous chapter, CBC and RSC contribute to a greater or lesser extent to the landscape of different CRC models. To assess the involvement of these populations in VG polyposis, fluorescent co-ISH for the CBC marker *Lgr5* and the

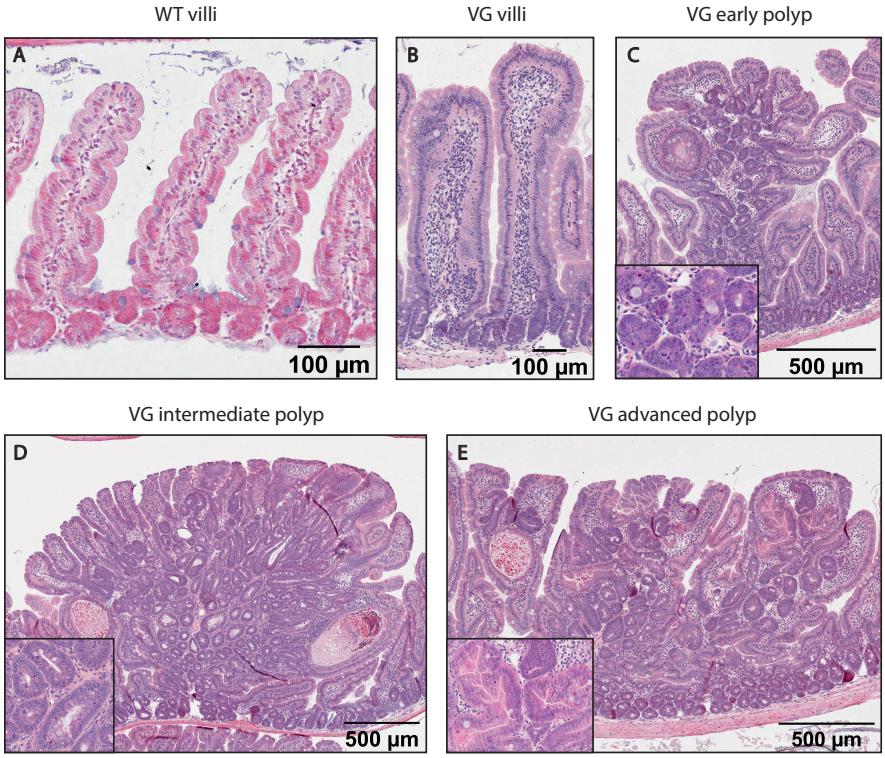

Figure 13: Histopathology of the Vil1-*GREM1* mouse model versus a WT animal. A. H&E of the small bowel villi of a WT animal. B-E. H&E of transformed villi (B), early (C), intermediate (D) and advance polyps (E) of a Vil1-*GREM1* mouse. Details show ectopic crypts.

RSC marker *Anxa1* was performed in Paraffin-embedded sections of VG intestines. Samples were collected 31-38 weeks after birth, a time by which VG intestines are heavily transformed[132]. Surprisingly, over 99 per cent of the ECF within stained polyps were double negative for *Lgr5* and *Anxa1* (Fig.14), suggesting that the origin of VG polyposis does not rely on the populations of cells described in Chapter 3, and that an alternative progenitor/stem cell population may drive tumorigenesis in this model (Fig.1).

4.5 Grem1 Antibody Treatment Reverts the VG Phenotype

The fact that HMPS is initiated by the upregulation of a secreted morphogen opens the door to therapeutic intervention using blocking antibodies. The utility of this

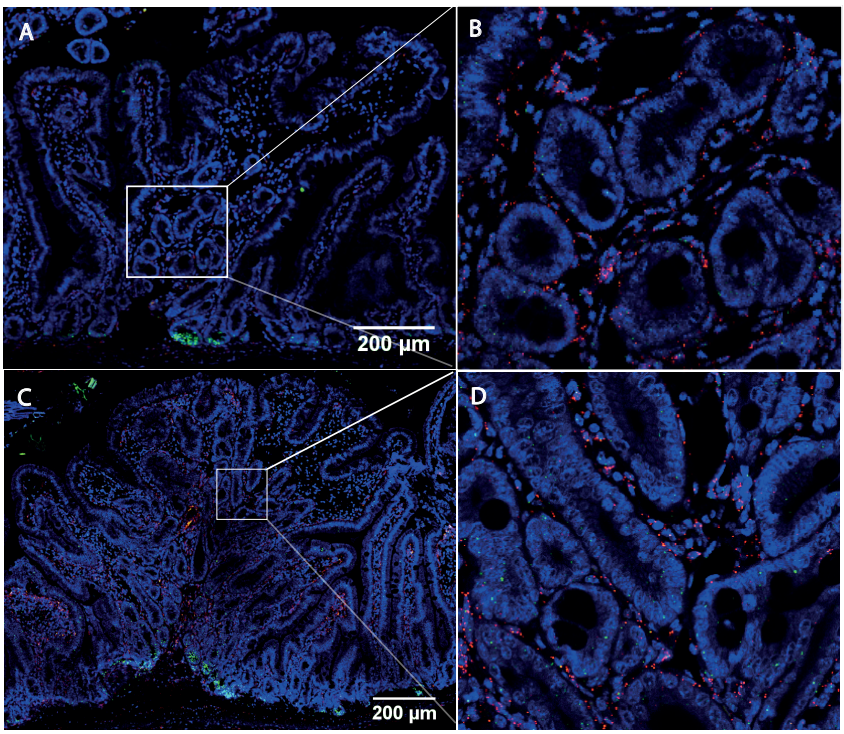

Figure 14: Fluorescent co-stain for the CBC marker *Lgr5* and the RSC marker *Anxa1* in Vil1-*GREM1* polyps. A,C. *In Situ Hybridisation* for *Lgr5* (green) and *Anxa1* (red). Details show ectopic crypts (B,D).

strategy was tested by subcutaneously injecting VG animals weekly with 30mg/kg of a Gremlin-1 blocking antibody (provided by UCB) from an age of 6 weeks and for a total of 6 weeks, a time by which samples were collected and stained with Hematoxylin and Eosin (H&E). This regime completely reversed the polyposis observed in VG animals, and the intestinal microscopic architecture reverted back to near normal (Fig.15A-B). These results establish this therapeutic agent as a good candidate to test in clinical settings for prevention of HMPS disease.

In order to investigate the efficacy of the Gremlin-1 blocking antibody in more advanced settings, animals were allowed to age for 21 weeks before being provided with the same therapeutic regime. This time, samples were collected after one, two, four, six and ten weeks of treatment, and H&E stains of these samples were used to quantify the differences in intestinal length, polyp size and number (Fig.15C,D). The effects of the Gremlin-1 blocking antibody in the small bowel area could be seen from week 1, a time by which this parameter was significantly smaller in treated animals than in controls (Fig.15G). Furthermore, colon area, polyp size and number were consistently lower after 4 weeks of treatment (Fig.15E,F,H). However, from this

time on, the phenotype of the treated animals remained stable, with no significant differences in number and size of polyps between samples treated for four versus ten weeks. Furthermore, by week 10, the intestines of these animals still presented with polyps (Fig.15C), suggesting that, at late stages of VG transformation, some of the lesions may have evolved mechanisms that render them independent of Gremlin-1.

4.6 Absence of Cell-Intrinsic WNT Mutations in VG Polyps

WNT disruption is an initiating event in the majority of colorectal malignancies, but whether this is a requirement in BMP-driven transformation reminds to be determined. Nuclear translocation of β-catenin is a hallmark of Wnt activation which is normally restricted to Lgr5+ cells at the base of the crypt, but can also be observed in malignant settings [39]. Here, IHC for β-catenin was used to assess the cellular localization of this protein within VG polyps as a read-out of Wnt activity. Over 99 per cent of the polyps had membranous β-catenin staining (Fig.16A), which correlated with a lack of *Lgr5* expression (Fig.16B).

In order to assess the presence of Wnt-disrupting mutations in these lesions, Whole-Exome-Sequencing (WES) and RNAseq were performed in a subset of small bowel polyps collected within 8 and 13 weeks after birth. DNA and RNA samples were extracted from fresh-frozen tissue and processed by the Genomic facilities in the Wellcome Center for Human Genetics. Regarding WES data, variant calling and post-processing were conducted by Ryan Schenk (a DPhil student within the Leedham laboratory) at the Wellcome Center for Human Genetics. The number of mutations across the analysed samples ranged between 16 and 211, but no hits in recognised CRC driver genes (as defined in Table.2.5 -Chapter 2-) were found in any of the polyps with membranous β-catenin stain, suggesting that no cell-intrinsic events were fuelling VG transformation in these lesions. Raw RNAseq reads were processed using *STAR-fusion* to look for fusions in *Rspo* genes, but none were found. Overall, no WNT-related alterations were detected in the samples of interest. Based on this evidence, we concluded that cell-intrinsic disruption of the WNT pathway was not required to sustain ECF progenitors or initialisation and propagation stages of intestinal polyposis in VG animals.

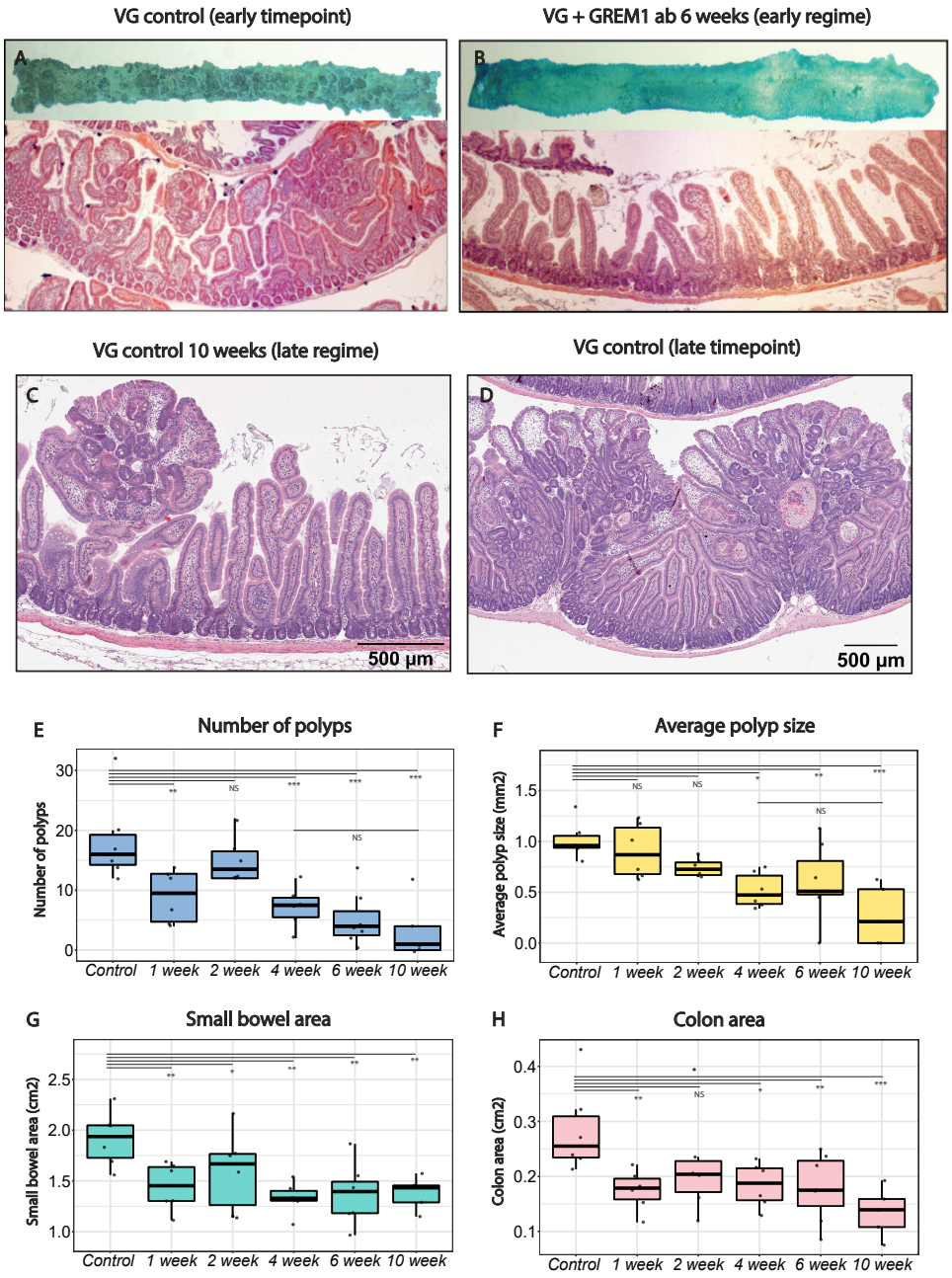

Figure 15: Treatment with a Gremlin-1 blocking antibody reverts the Vil1-*GREM1*(VG) phenotype. A,B. H&E of a the small bowel of an VG treated with a Gremlin-1 blocking antibody from an early time-point(B) versus a paired untreated control(A). C,D. H&E of a the small bowel of an VG treated with a Gremlin-1 blocking antibody from a late time-point(C) versus a paired untreated control(D). E-H. Boxplots representing the number of polyps(E), average polyp size(F), small bowel area(G) and colon area(H) of VG animals treated with a Gremlin-1 blocking antibody from a late time-point for 1,2,4,6 and 10 weeks versus untreated controls. Statistical analysis was conducted using a pairwise t-test. P-value was corrected using the Bonferroni method. Asterisks indicate a p-value <0.05 (*), <0.01(**), <0.001 (***) or >0.05 (NS).

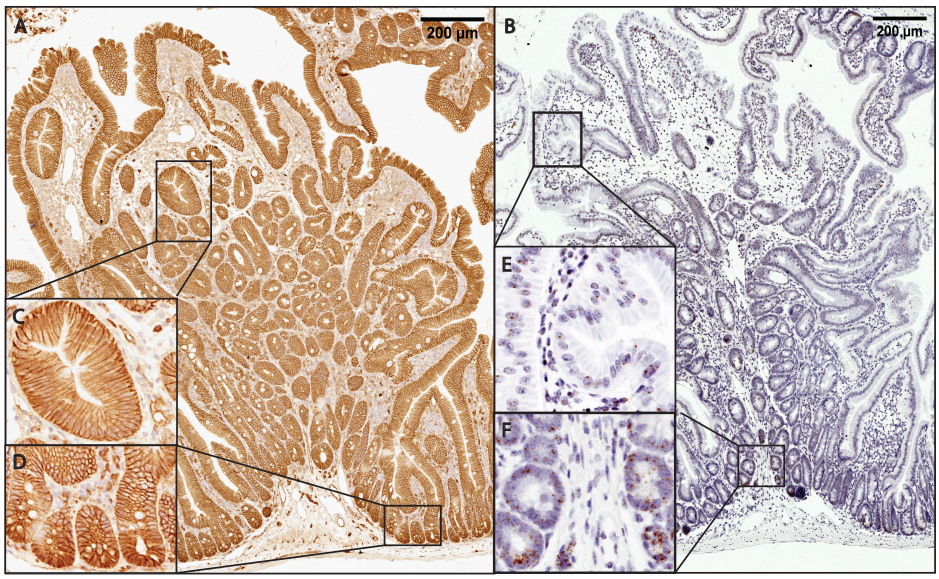

Figure 16: Vil1-*GREM1* polyps do not show signs of strong Wnt activation. A,C,D. β-catenin immunohistochemistry. B,E,F. Lgr5 *In Situ Hybridisation*. Details show conventional (D,F) and ectopic (C,E) crypts

4.7 Environmental Sources of WNT in VG Polyps

Despite the lack of cell-intrinsic WNT activation observed in the majority of VG samples, dysregulation of Wnt ligands could potentially be involved in the maintenance of ECF progenitors. To assess the expression of Wnt and R-spondin ligands in the VG model, RNAseq from VG polyps and WT small bowel was performed. Among the ligands analysed, the levels of *Wnt1* and *Wnt16* were too low and these genes were filtered out. The results revealed that the expression levels of Wnt and R-spondin ligands did not differ to a great extend between WT and VG tissues (Fig.17A). The only ligand that was significantly upregulated between VG and WT samples was *Wnt11*, but this transcript was undetectable in most VG polyps by ISH (Fig.17B).

Bulk RNA sequencing is able to quantify differences in whole tissue ligand expression but is unable to determine the spatial distribution of the transcripts, which is critical to maintain polarised gradients of WNT activity along the crypt-villus axis. Key Wnt ligands (eg. Wnt2b, Wnt5a, R-spondin3) are expressed by populations of fibroblasts within the intestinal niche [49, 50, 51]. Specifically, Gli+ fibroblasts have been reported to secrete Wnt2b, whereas Foxl1+ telocytes are an established source of Wnt5a [49, 50, 51]. Given that *Wnt5a* tended to be upregulated in VG samples, ISH for this transcript was performed to assess its spatial distribution, which revealed a clear upregulation of *Wnt5a* in stromal cell populating the edges of the

polyps (fig.18C).

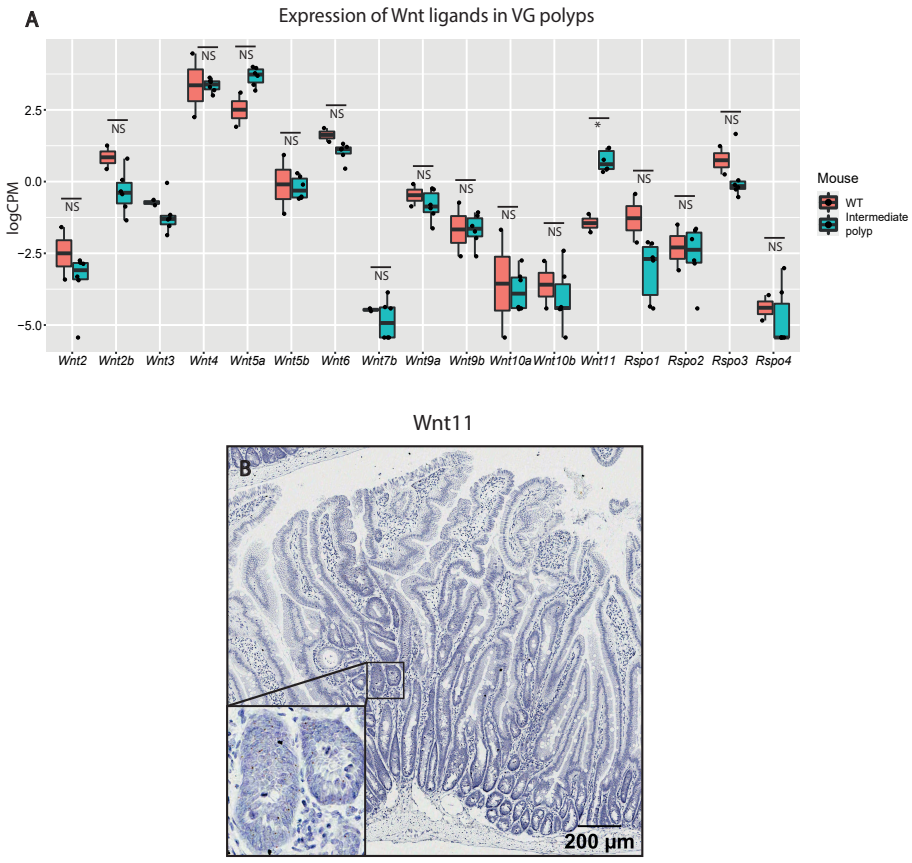

Figure 17: Differences in the transcription of Wnt and Rspo ligands between Vil1-*GREM1* and WT animals. A. Boxplot showing the log-transformed normalized counts for Wnt and R-spondin ligands expressed in villi of Vil1-*GREM1* and WT animals. Statistical analysis was conducted using a pairwise t-test. P-value was corrected using the Bonferroni method and represented as asterisks indicating a p-value <0.05 (*), <0.01(**), <0.001 (***) or >0.05 (NS). B,C. *In Situ Hybridisation* for *Wnt11* (B) and *Wnt5a* (C) in Vil1-*GREM1* polyps.

Following this lead, the expression of other ligands secreted by niche populations, namely *Wnt2b* and *Rspo3*, was assessed by ISH. In WT animals, expression of *Wnt2b* and *Rspo3* was confined to populations of fibroblasts at the base of the crypts, whereas *Wnt5a* was restricted to telocytes lining the sides of the villi, as reported by Shoshkes-Carmel et al [49] (Fig.18A,D,G). Interestingly, untransformed VG villi already showed increased levels of *Wnt2b* and *Wnt5a* transcripts, while *Rspo3* retained its homeostatic pattern of expression (Fig.18B,E,H). In polyps, *Wnt2b* showed a very distinct localization from *Wnt5a*. Instead of being expressed at the edge of the lesions, its expression localized to the stromal surrounding ECF (Fig.18F). Moreover, moderate

levels of *Rspo3* transcripts were observed in this same region (Fig.18I). The focal expression of these transcripts explains why they did not appear to be upregulated in bulk transcriptomic samples of VG mice.

Furthermore, fluorescent ISH was used to study the co-localization of *Gli/Foxl1* and *Wnt2b/Wnt5a* within VG polyps. As expected, *Gli* and *Wnt2b* were co-expressed by populations of cells surrounding the ECF, whereas *Foxl1* and *Wnt5a* signals were co-detected at the edges of the polyps (Fig.19). Overall, this evidence suggests that aberrant epithelial expression of Gremlin-1 leads to activation of fibroblast populations able to produce ectopic Wnt ligands.

Finally, the effect of a the GREM1 blocking antibody on the upregulation of Wnt ligands was assessed by ISH. Interestingly, the expression levels of *Wnt2b* and *Wnt5a* were decreased in antibody-treated samples with respect to non-treated controls (Fig.20), reaching levels comparable to those found in WT tissues. This suggests that the stromal reprogramming initiated by Gremlin-1 can be reverted upon re-establishment of the homeostatic morphogenic gradients.

4.8 Porcupine Inhibition Reverts Polyposis in VG Animals

Environmental Wnt ligands are essential to sustain homeostatic crypts [49, 50, 51]. Hence, the functional contribution of Wnt ligands (i.e. *Wnt2b* and *Wnt5a*) to ECF maintenance and proliferation was assessed. In order to investigate this, VG animals were administered 5 mg/kg of Porcupine inhibitor (LGK974) via oral gavage two times per day, from day 45 to day 120 after birth, and sampled on the final day of the treatment by Owen Sansom's team in the Beatson Center. This therapeutic regimen reduced the number of polyps and Ki67+ proliferative cells in the treated animals versus the controls, but unlike the Gremlin-1 blocking antibody, did not revert the abnormal villus architecture phenotype (Fig.21). As happened with the Gremlin-1 blocking antibody, some lesions were resistant to Porcupine inhibition. These results support a role for cell-extrinsic Wnt ligands in the propagation of lesions in Vil1-*GREM1* polyposis.

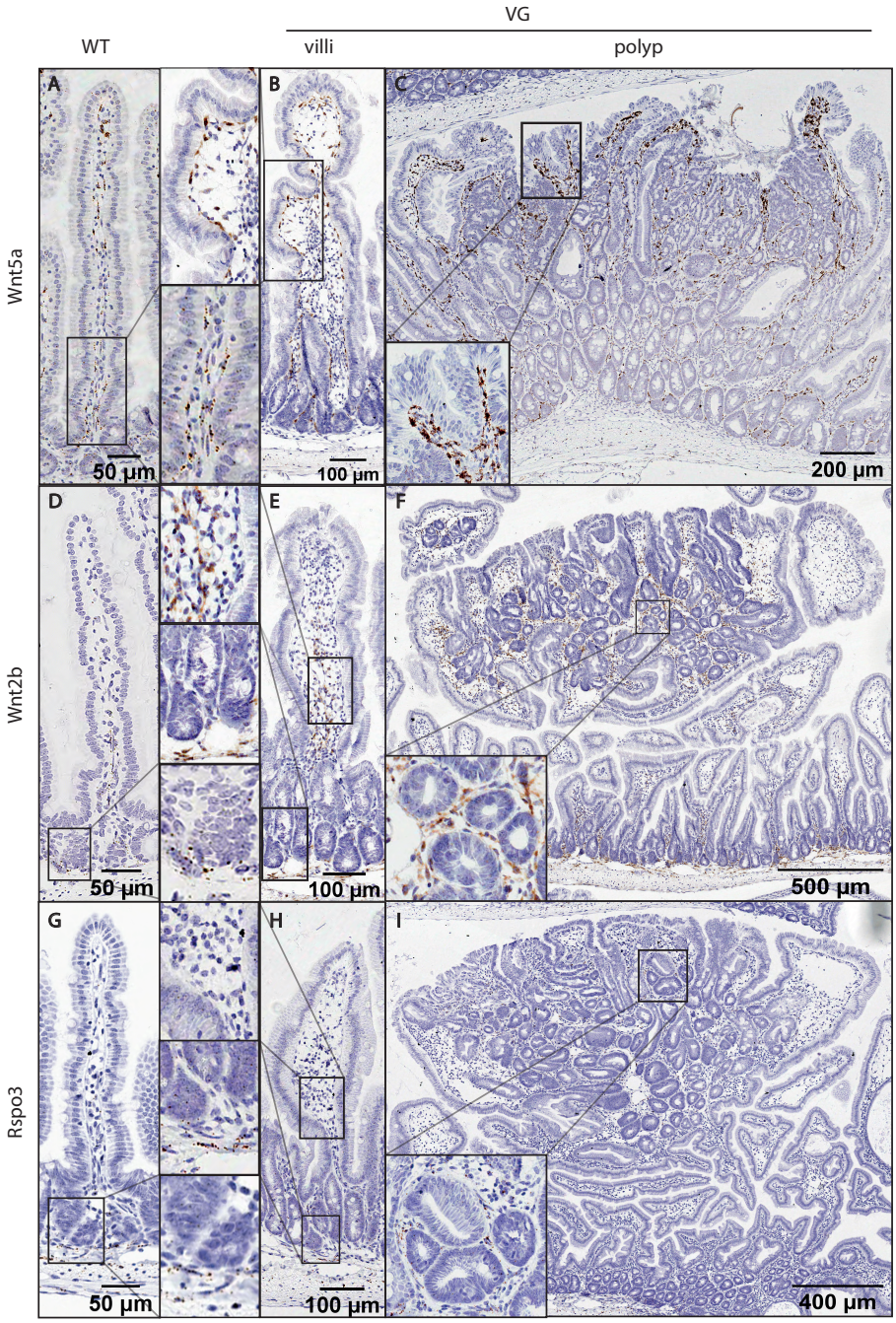

Figure 18: Expression of *Wnt2b, Wnt5a* and *Rspo3* in WT and Vil1-*GREM1* animals. A-I.*In Situ Hybridisation* of *Wnt5a* (A,B,C), *Wnt2b* (D,E,F) and *Rspo3* (G,H,I) in crypt-villus units from WT(A,D,G) and Vil1-*GREM1* animals(B,E,H) as well as Vil1-*GREM1* polyps (C,F,I). Details show a close-up of the villi walls (A,B,E,H), polyp walls (C), conventional crypts (D,G) and ectopic crypts (C,I).

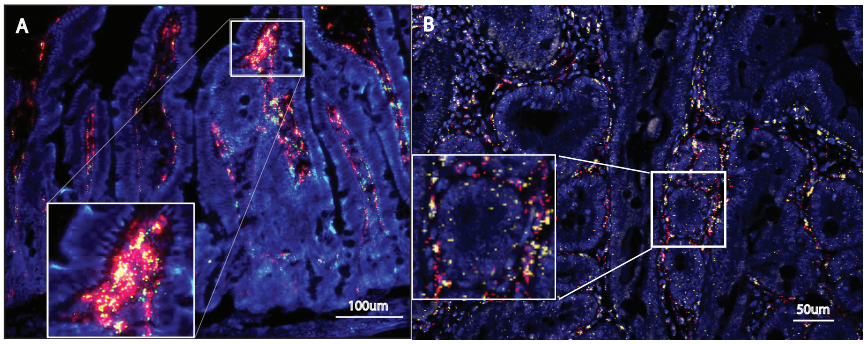

Figure 19: *Wnt2b* and *Wnt5a* are co-expressed with the fibroblast markers *Gli* and *Wnt5a* respectively. Co-*In Situ Hybridisation* for *Foxl1*(green) and *Wnt5a*(red) in Vil1-*GREM1* villi. Detail shows a close-up of the tip of a villus. H. *In Situ Hybridisation* for *Gli*(yellow) and *Wnt2b*(red) in a Vil1-*GREM1* polyp. Details shows a close-up of an ectopic crypt.

4.9 The Non-Canonical WNT Receptor Frizzled-5 is Profoundly Up-regulated in VG Polyps

The effect of Porcupine inhibition implicated a cell-extrinsic, ligand-dependent effect of Wnt in VG polyposis. Once this had been established, a new question arose: through which receptors do ectopic crypt epithelial cells sense the stromal Wnt? In homeostasis, Lgr5+ ISC express *Fzd7*, whereas *Fzd5* is normally restricted to the TA area within the crypt-villus axis [237]. To assess the Frizzled receptor expression landscape in the VG model, RNAseq from VG polyps and WT small bowel was performed. Interestingly, *Fzd5* was found to be consistently upregulated in VG polyps with respect to WT controls (Fig.22A), whereas the levels of *Fzd7* remained unchanged. Chromogenic ISH for *Fzd5* confirmed a clear increase of this transcript in VG polyps and untransformed villi with respect to WT controls (Fig.22B-H).

4.10 Escaper Cells Repopulate the Polyps of VG-VilER-Cre-Fzd5KO$^{-/-}$ Animals

Having identified aberrant Fzd5 expression in VG mice with profound upregulation in the ectopic crypts, it was hypothesised that this receptor might be functionally important in signal transduction of the ectopic Wnt ligands. To assess this, knockout (KO) models were used to deplete *Fzd5* in VG animals. In parallel, *Fzd7* KO

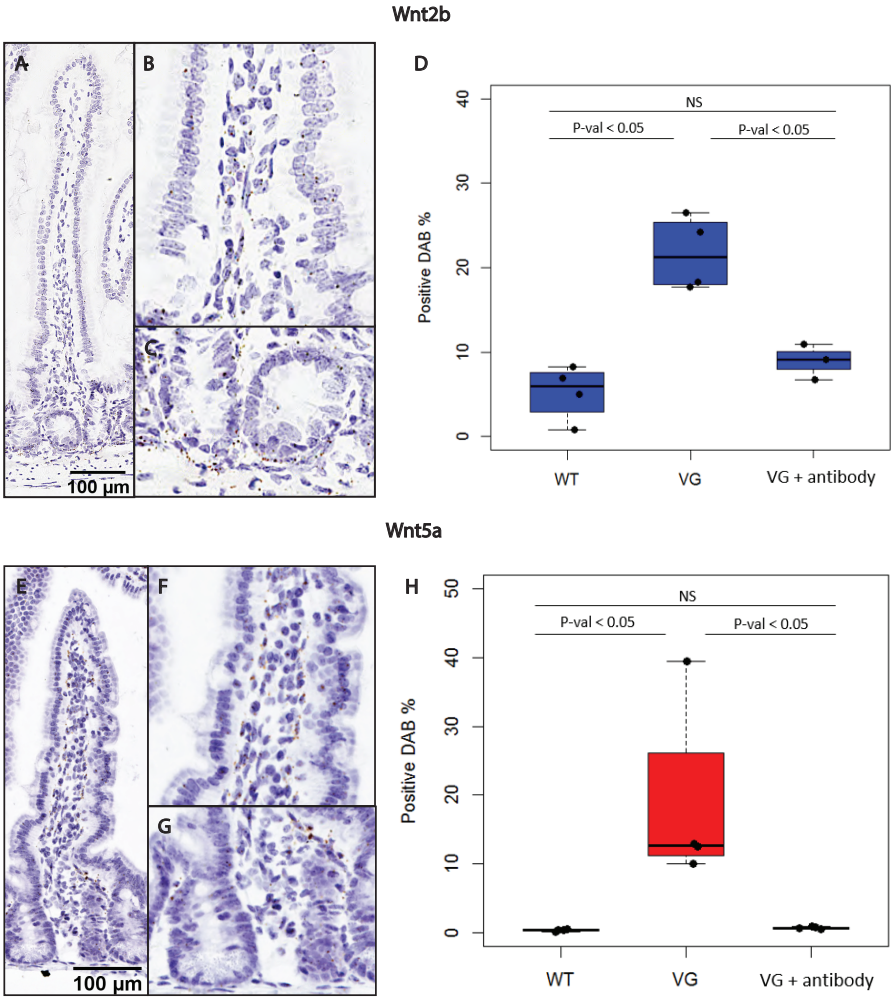

Figure 20: Treatment with a Gremlin-1 blocking antibody restores the levels of expression of Wnt ligands. A-C, E-G. *In Situ Hybridisation* for *Wnt2b* (A-C) and *Wnt5a* (E-G) along the crypt-villus axis of Vil1-*GREM1* animals. Details show a close-up of the villi wall (B, F) and conventional crypts (C, G). D,H. Quantification of the levels of expression of *Wnt2b*(D) and *Wnt5a*(J) was performed using the Image Analysis Software QuPath[220]. Statistical significance was tested using a pairwise t-test. P-value was corrected using the Bonferroni method and represented as asterisks indicating a p-value <0.05 (*), <0.01(**), <0.001 (***) or >0.05 (NS).

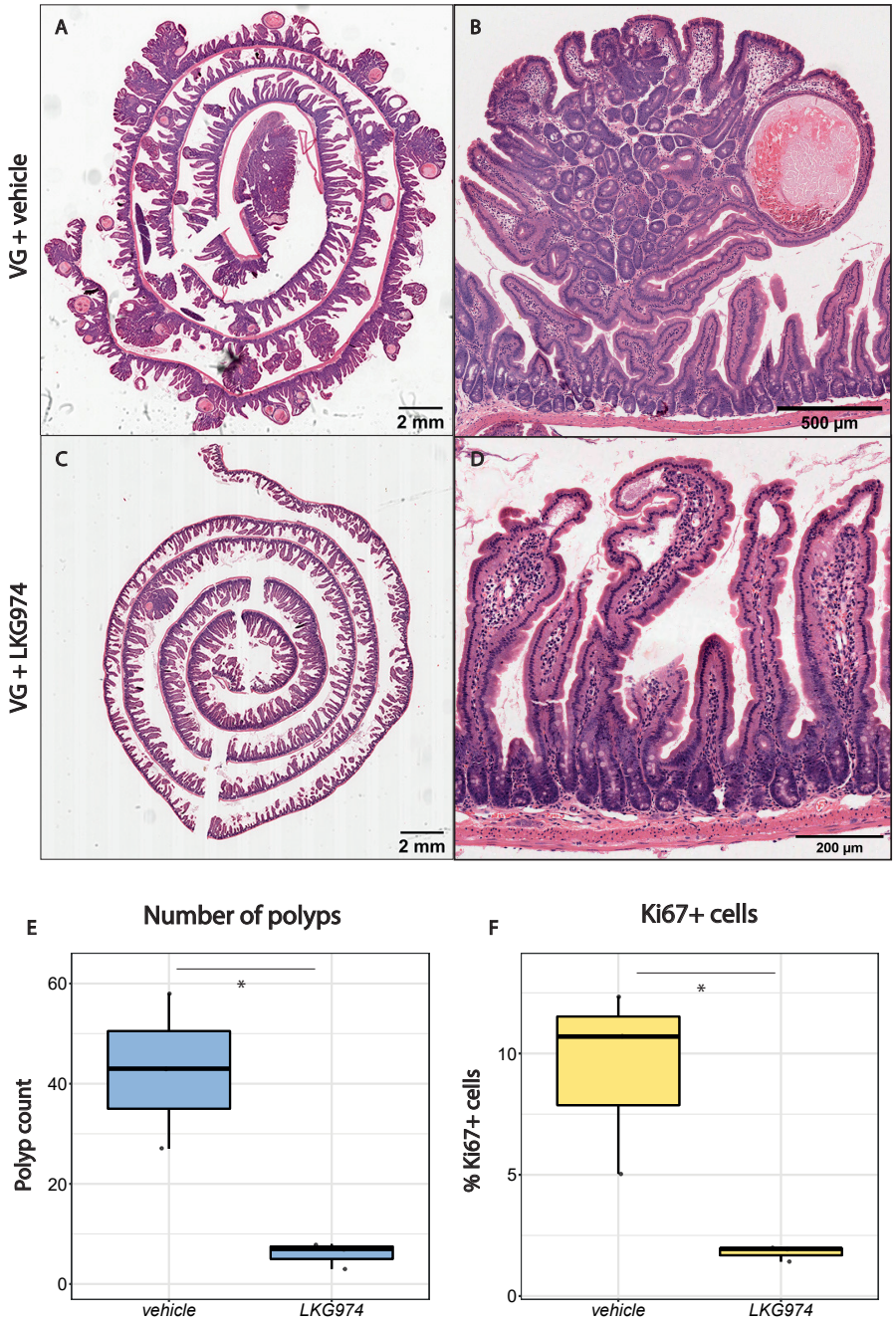

Figure 21: Treatment with a Porcupine inhibitor partially reverts the phenotype of Vil1-*GREM1*(VG) animals. A,C. Gut roll of the small bowel from a VG animal treated with vehicle (A) or LKG974 (C). B,D. Close-up of the gut rolls showing the polyp of a control VG mouse (B) and the abnormal villi of a control VG animal (D). E,F. Boxplots showing the number of polyps (E) and Ki67+ cells (F) in VG animals treated with vehicle versus LKG974. Quantification of the number of Ki67+ cells was performed using the Image Analysis Software QuPath[220]. Statistical significance was tested using a two-sides t-test. Asterisks indicate a p-value <0.05 (*), <0.01(**), <0.001 (***) or >0.05 (NS).

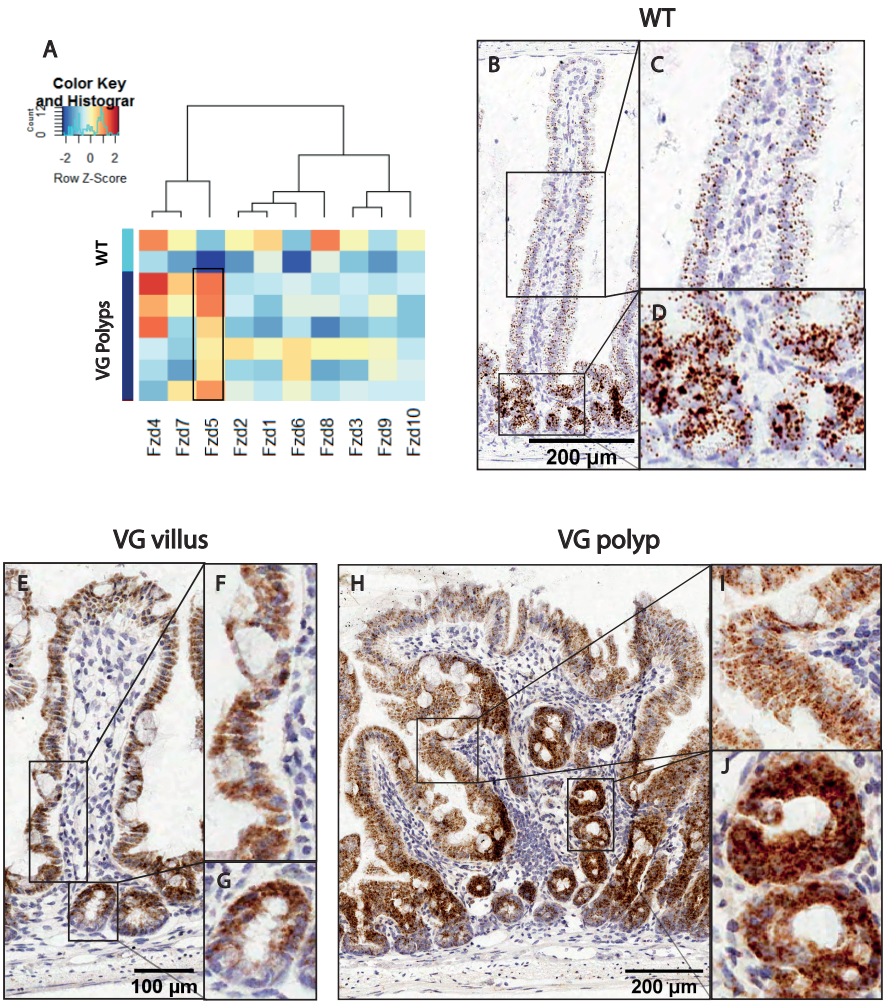

Figure 22: *Fzd5* is upregulated in the epithelium of Vil1-*GREM1* animals. A. Heatmap showing the log-transformed normalized counts of Frizzled transcripts in WT villi versus Vil-GREM1 polyps. B-J. *In Situ Hybridisation* for *Fzd5* in WT (B,C,D) and Vil-GREM1 (E-J) samples. Details show villi (C,F), conventional crypts (D,G) and ectopic crypts (J).

models were generated to assess how disruption of the canonical Wnt receptor in Lgr5+ cells affected VG pathogenesis.

To start with, $Fzd5^{tm2Nat/J-/-}$ and $Fzd7^{-/-}$ mice (Fzd5KO and Fzd7KO respectively) were crossed with $C57BL/6J^{(Vil1\text{-}cre/ERT2)23Syr}$ (VilER-Cre) to obtain VilER-Cre-$Fzd5KO^{-/-}$ and VilER-Cre-$Fzd7KO^{-/-}$ animals respectively. This allowed for conditional deletion of these genes in the intestinal epithelium upon tamoxifen injection. First, the levels of KO were assessed 7 days post-injection. By that time, *Fzd7* expres-